Supporting Information

Formation of Self-assembled Multi-layer Stable Palladium Nanoparticle for Ligand-free Coupling Reactions

Mitsuhiro Arisawa[1]*, Mohammad Al-Amin[1], Tetsuo Honma[2], Yusuke Tamenori[2], Satoshi Arai[3], Naoyuki Hoshiya[1, 2], Takatoshi Sato[1], Mami Yokoyama[4], Akira Ishii[4], Masaki Takeguchi[5], Tsuyoshi Miyazaki[5], Masashi Takeuchi[3], Tomohiro Maruko[3], Satoshi Shuto[1]

[1] Faculty of Pharmaceutical Sciences, Hokkaido University, Kita-12, Nishi-6, Kita-ku, Sapporo 060-0812, Japan.

[2] Japan Synchrotron Radiation Research Institute, 1-1-1 Kouto, Sayo-cho, Sayo-gun, Hyogo 679-5198, Japan.

[3] Furuya Metal Company Limited, Minami-otsuka 2-37-5, Toshima-ku, Tokyo 170-0005, Japan

[4] Graduate School of Engineering, Tottori University, 101, Minami 4-chome, Koyama-cho, Tottori 680-8550, Japan

[5] National Institute for Materials Science, Address: 1-2-1 Sengen, Tsukuba 305-0047, Japan

Fig. S1. Effect of ligands in Pd catalyzed aromatic amination.

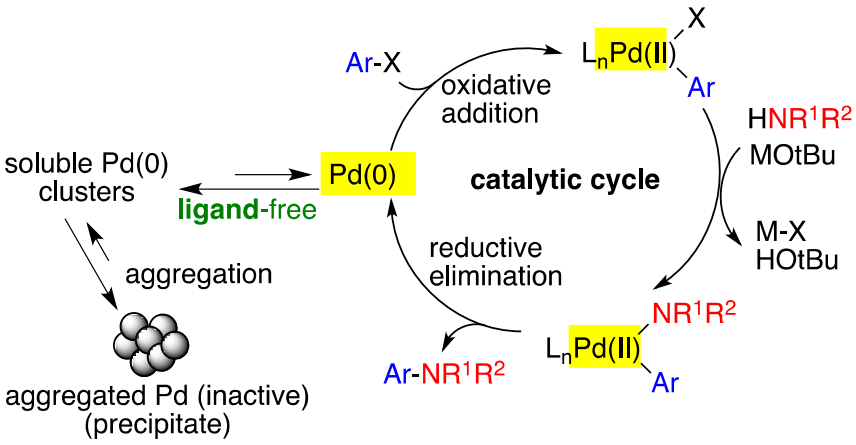

Fig. S2. STEM-EELS line profile.

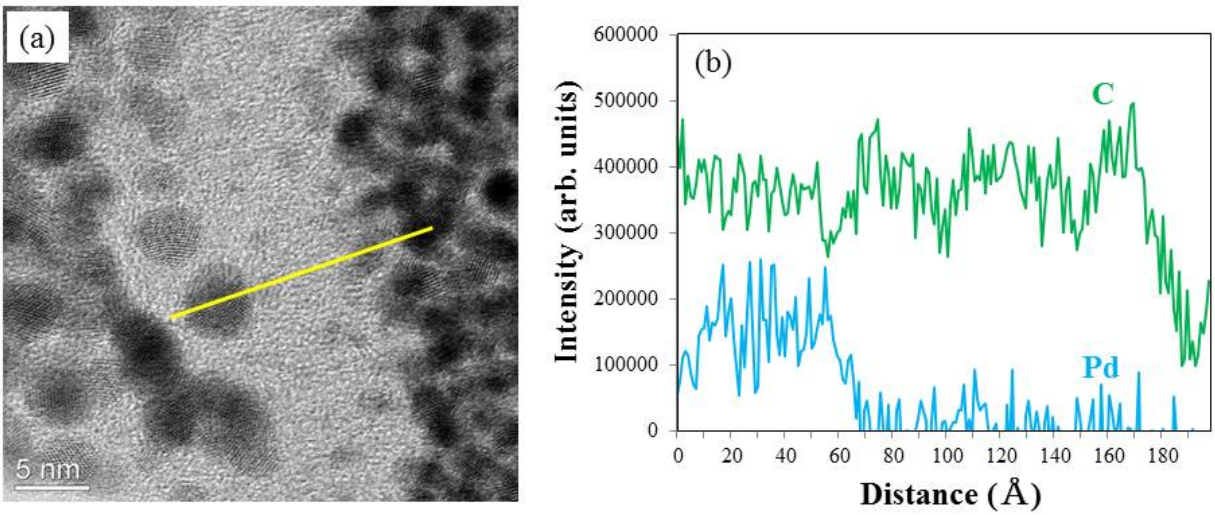

The 5 nm size of nanoparticle and matrix between nanoparticles are palladium and carbon, respectively. Sulfur surrounds palladium.

Fig. S3. (a) Pd K-edge $k^3\chi(k)$ EXAFS oscillations spectra of SAPds and Pd foil. (b) Pd-K edge Fourier transforms of $k^3\chi(k)$ EXAFS oscillations spectra in the k range of 2.0 – 10.5 Å $^{-1}$ of SAPds, SM product and Pd foil. The inset shows Fourier transforms of EXAFS oscillation spectra in the k range of 2.0 – 6.5 Å $^{-1}$ of Pd foil, SAPd before and BH product.

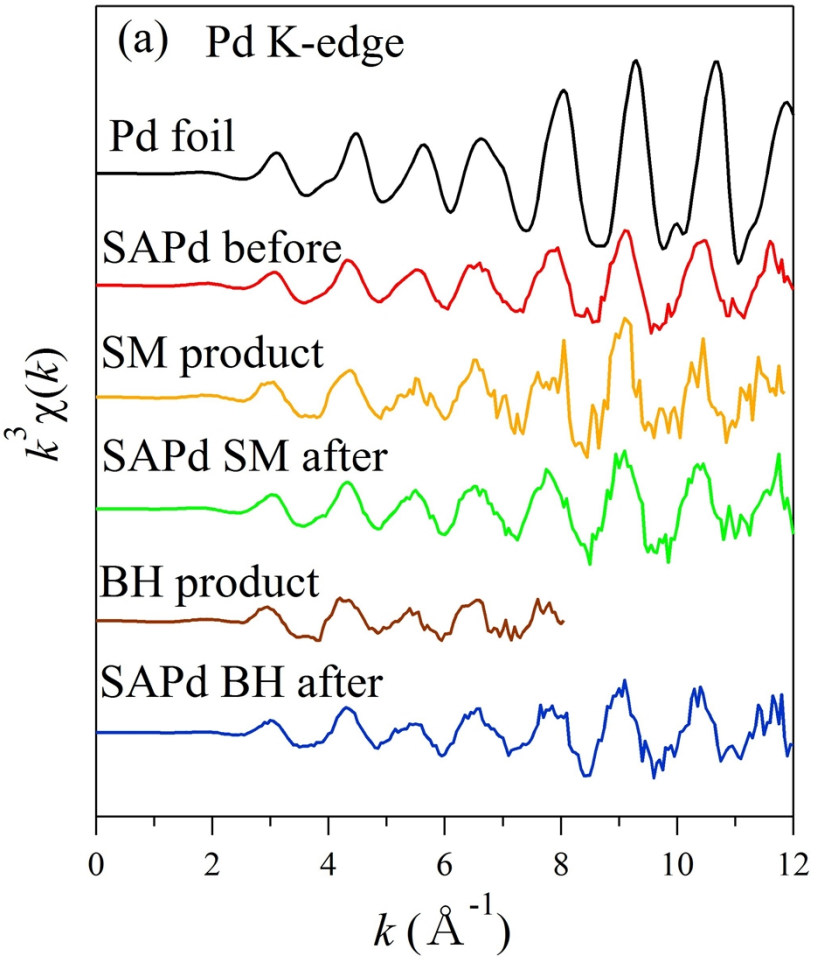

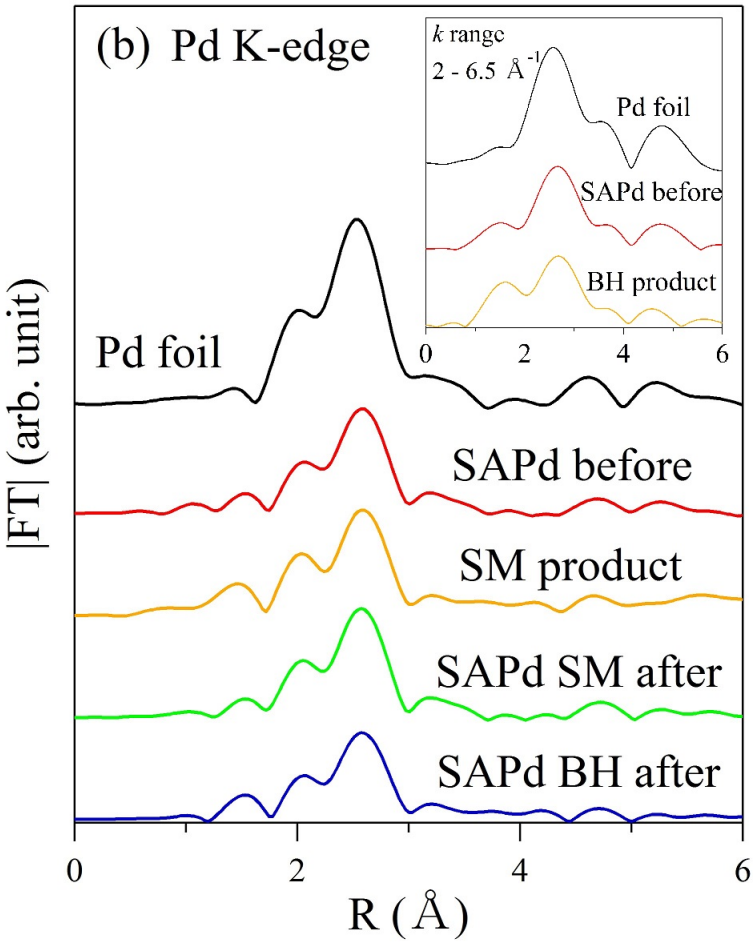
(b) Pd K-edge
k range
2 - 6.5 Å-1
Pd foil
SAPd before
BH product
0
2
4
6
Pd foil
SAPd before
SM product
SAPd SM after
SAPd BH after
|FT| (arb. unit)
0
2
4
6
R (Å)

Fig. S4. C K-edge XANES spectra of SAPd before and standard materials.

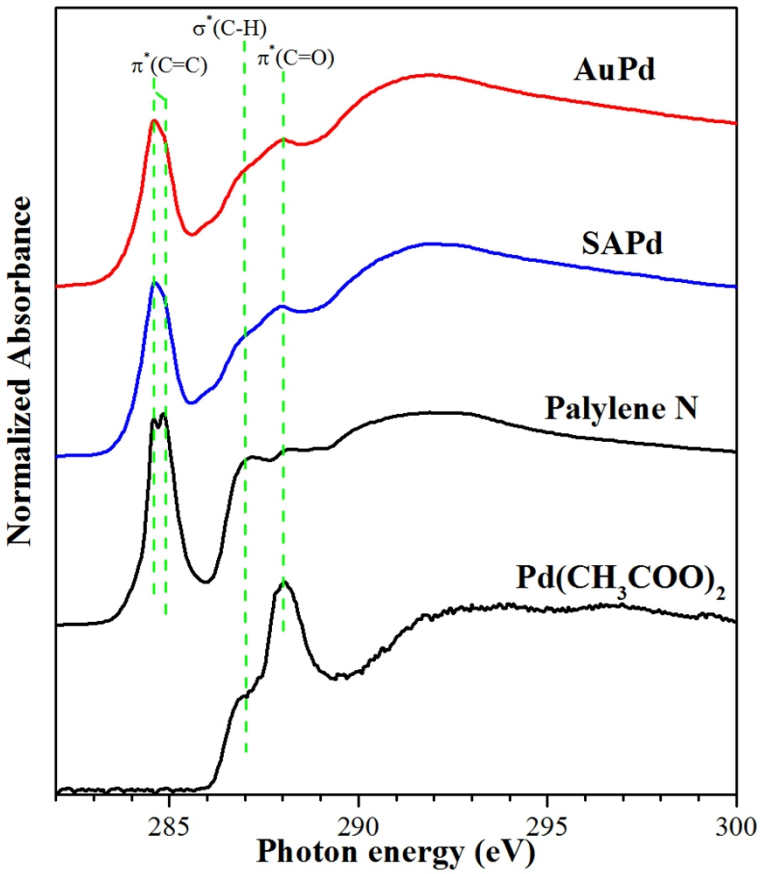

Fig. S5. Release and catch mechanism of SAPd.

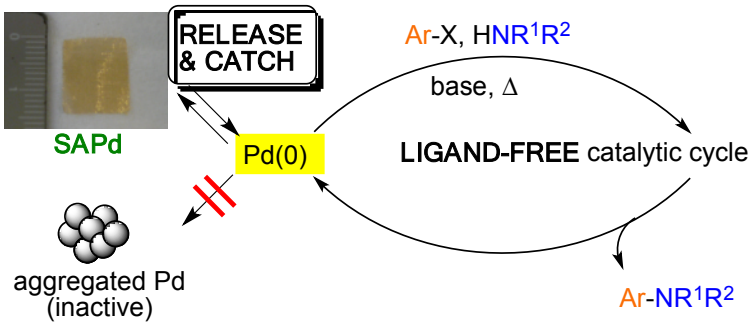

Preparation of sulfur modified gold supported Pd material (SAPd)[1]

The Au (100 mesh-14 × 12 mm^2) was placed in the piranha solution [prepared *in situ* by 35 % H_2O_2 aqueous solution (1.0 mL) and concentrated H_2SO_4 (3.0 mL)] for 5 min and then washed first by H_2O (3.0 mL × 10) and then with EtOH (3.0 mL × 6). The Au-mesh was placed in a round bottom flask and dried for 10 min under reduced pressure (*ca*. 6 mm Hg). The resulting sulfur-modified Au was placed in a solution of $Pd(OAc)_2$ (5.3 mg, 0.023 mmol) in xylene (3.0 mL) and stirred at 100 °C for 12 h under the Ar atmosphere. Then the plate was rinsed with xylene (3.0 mL × 50) and after vacuum drying, it was placed in xylene (3.0 mL) and heated at 135 °C for 12 h. Finally, the plate was rinsed with xylene (3.0 mL × 50) and dried under vacuum for 10 min to give sulfur modified gold supported Pd material (SAPd).

TEM experiment

For Fig. 2;

A layer of carbon was applied to the sample surface and then platinum was FIB-deposited by injection of an organo-metallic gas and then rastering the 30kV gallium ion beam over the area of interest. A thin cross section measuring approximately 25 µ long, 2 µ wide and 8 µ deep was extracted from the die surface using a proprietary in-situ FIB technique. The cross section was attached to a 200 mesh copper TEM grid using FIB-deposited platinum. One electron transparent window was thinned to electron transparency using the gallium ion beam of the FEI FIB.

The TEM grid with the foil was transferred to a Tecnai TF-20 scanning transmission electron microscope. Transmitted electron images were acquired at various magnifications in bright-field, high-resolution and high angle annular dark field mode (HAADF). The elevant instrument settings used during image acquisition are given in Table S1.

Instrument	Transmission Electron Microscope
Manufacturer/Model	FEI Tecnai TF-20 TEM/STEM
Accelerating Voltage	200kV
Condenser Aperture	#2
Objective Aperture	#3
Objective Lens Current	1.438

Table S1. Instrument Settings for imaging system used on sample.

For Fig. 3, S2;

A layer of carbon was applied to the sample surface and then platinum was FIB-deposited by injection of an organo-metallic gas and then rastering the 30kV gallium ion beam over the area of interest. A thin cross section measuring approximately 25 µ long, 2 µ wide and 8 µ deep was extracted from the die surface using a proprietary in-situ FIB technique. The cross section was

attached to a 200 mesh copper TEM grid using FIB-deposited platinum. One electron transparent window was thinned to electron transparency using the gallium ion beam of the FEI FIB.
The TEM grid with the foil was transferred to a JEOL JEM-ARM200F© transmission electron microscope equipped with probe-forming and imaging optics aberration correctors operated at 200 kV. Transmitted electron images were acquired by bright field (BF) and high angle annular dark field (HAADF) scanning transmission electron microscopy (STEM). STEM-Electron energy loss spectroscopy (EELS) was performed using Gatan Enfina1000© attached to the bottom of the microscope. The relevant instrument settings used during image acquisition and EELS analysis are given in Table S2.

Instrument	transmission electron microscope
Manufacture/Model	JEOL JEM-ARM200F
Accelerating Voltage	200kV
Condenser Aperture	40μmφ
Objective Aperture	Not used
Objective Lens Current	Unknown

Table S2. Instrument Settings for imaging system used on sample.

XAFS experiments

For Figs. S3 and S4;

The X-ray absorption fine structure (XAFS) measurements were performed at hard X-ray beamline BL14B2 of SPring-8 in Japan.[3] The incident hard X-rays were obtained using a silicon double crystal monochromator from synchrotron radiation from the 8GeV storage ring. The net plane is (311) for the Pd K-absorption edge. The higher harmonics of the incident X-rays were reduced using two Rh-coated mirrors. The spectra of standard materials (Pd foil, PdO, $PdSO_4$, PdS and $Pd(PPh_3)_4$) were taken in the normal transmission mode. The spectra of SAPd before the 10^{th} cycle of the optimized Suzuki-Miyaura and Buchwald-Hartwig cross couplings (SAPd before), and after the 10^{th} cycle of the optimized Suzuki-Miyaura (SAPd SM after) and Buchwald-Hartwig cross couplings (SAPd BH after), crude Suzuki-Miyaura coupling product (SM product) and crude Buchwald-Hartwig product (BH product) were measured in the fluorescent X-ray yield method using a 19-elements Ge solid state detector. All the measurements were done at room temperature. The XAFS spectra were analyzed by ATHENA and ARTEMIS XAFS analysis package.[4] For all measurements, data analysis to remove the background and qualitatively analyze the XANES was carried out manually. The data were normalized for variations in the primary X-ray intensity. A

linear pre-edge was removed for each spectrum and the data were normalized by the height of the edge-jump. The theoretical scattering amplitude and phase shift function of the single scattering path was calculated by FEFF6. [5]

Fig. S3(a) shows Pd K-edge XANES spectra of SAPd before and standard materials. The XANES spectrum of SAPd before is similar to that of Pd foil. It suggests that the valence state of Pd on SAPd is almost zero that is metallic like Pd metal. Fig. S3(b) also shows Pd K-edge XANES spectra of SAPd before and, SAPd SM after, SAPd BH after, SM product and BH product. Those spectra of SAPds SM/BH after and SM/BH products are identical to that of SAPd before. It is concluded that the chemical state and local structure of Pd on SAPd do not change after the cross couplings and the states of Pd that remained in the product is also the same. It is concluded that the active materials are metallic Pd particles.

Fig. S4(a) shows Pd K-edge $k^3\chi(k)$ EXAFS oscillations spectra of SAPd before, SAPd SM/BH after and SM/BH products and Pd foil. It is found that the amplitude of the EXAFS oscillation spectra of SAPds and SM/BH products are small compared to that of Pd foil, while the periods and the phases of the oscillations are almost same with that of Pd foil. These results suggest that metallic Pd particle on SAPds and in SM/BH products is nanoparticle. Fig. S4(b) shows Pd-K edge Fourier transforms of $k^3\chi(k)$ EXAFS oscillations spectra in the k range of 2.0 – 10.5 Å $^{-1}$ of SAPds, SM product and Pd foil. Fourier transforms of EXAFS oscillation spectra in the k range of 2.0 – 6.5 Å $^{-1}$ of Pd foil, SAPd before and BH product are shown inset of Fig. S4(b). To precisely investigate the size of the metallic Pd particles, theoretical curve fittings of EXAFS oscillations were performed for Pd-Pd peak in back Fourier transformed the wave number k space for the k and radial distance R ranges of 2 – 10.5 Å $^{-1}$ and 1.75 – 3.0 Å, respectively. Only for BH product, the k and R ranges are 2.0 – 6.5 Å $^{-1}$ and 2.0 – 3.4 Å, respectively. It is for this reason that the concentration of Pd in BH product is very low (< 1 ppm) and then the S/N of the EXAFS spectrum is considerably low. We only considered one single scattering path in the curve fitting analyses. The intrinsic loss factor S_0^2 was determined from Pd foil and held constant thereafter. The parameters determined by curve fitting analysis are listed in Table S2. In the case of SAPd before, the curve fitting analysis revealed the average CN of 8.6±0.9, which is smaller than that of Pd foil. Then the average size of Pd nanoparticle with a CN of 8.6±0.9 is estimated to be about 2-4 nm. [6, 7] From the average CNs for SAPds SM/BH after and SM/BH products, the average sizes of Pd nanoparticles are estimated to be also about 2-4 nm. The average size of Pd nanoparticles estimated by EXAFS curve fitting analysis was smaller than that obtained by TEM. This might be ascribed to the difficulty in finding small Pd nanoparticles (< 1 nm) by TEM.

Table S3. EXAFS fit parameters for Pd—Pd. Intrinsic loss factor, S_0^2 = 0.84 (Pd—Pd from Pd foil data).

	CN[a]	R[Å][b]	δ^2[Å^2][c]	E_0[eV][d]	R_{factor}[%][e]
Pd foil	12[f]	2.74±0.01	0.0056±0.0005	-0.3±0.6	0.1
SAPd before	8.6±0.9	2.79±0.01	0.0075±0.0007	-0.4±0.8	0.3
SAPd SM after	9.4±1.4	2.79±0.01	0.0078±0.0010	-1.6±1.1	0.5
SAPd BH after	7.4±1.1	2.80±0.01	0.0076±0.0010	-0.9±1.1	0.5
SM product	9.5±0.5	2.80±0.01	0.0075[g]	-2.4±1.2	1.0
BH product	8.1±1.7	2.83±0.07	0.0075[g]	-2.5±4.7	3.6

[a] First shell coordination number. [b] Interatomic distance. [c] Debye-Waller factor. [d] Correction of edge energy. [e] Goodness-of-fit index. [f] Coordination number was fixed as that of a fcc lattice. [g] Debye-Waller factor was fixed with the same value as the one of SAPd before.

For Figs. S5 and S6;

XANES analysis at sulfur and carbon K-edge were used to determine the chemical states of sulfur and carbon in SAPd. The detailed features of XANES spectrum directly measure the unoccupied orbitals of the element of interest in a sample [8], and it is a fingerprint reflecting the chemical state of the element in a complex. Detailed chemical information of SAPd can be deduced from the comparison between XANES spectrum of SAPd and existing literature on standard materials. The XANES analysis has been carried out using soft X-ray beamline BL27SU of SPring-8. BL27SU consists of two branches. The B-branch provides higher energy soft X-ray beam by use of a Si(111) double crystal monochromator. On the other hand, equipped with a varied-line-spacing plane grating monochromator, the c-branch provides lower soft X-ray radiation in the range from 170 to 2300 eV.

The chemical state of sulfur was analyzed by using b-branch of BL27SU. The radiation from the undulator was mohochromatized by using a double crystal Si(111) monochromator ensures an energy resolution of 0.35 eV. Photon flux on the sample is 1×10^{11} Ph/s at 2.5keV (sulfur K-edge). XANES spectra were measured by scanning the undulator gap as well as the monochromator scan to maintain maximum intensity of the incident soft X-rays. For XANES measurements, SAPd samples were fixed onto a sample holder by screws, and powdered standard materials were fixed on the sample holder by double sided carbon tape. The sample holder was fixed on a linear and rotatable manipulator and installed in an analysis chamber. The pressure of analysis chamber was 1Pa. XANES spectra of SAPd and standard materials were recorded by partial-fluorescence yield (PFY) method by using a silicon drift detector (SDD) [9]. The SDD was mounted perpendicular to the axis

of the incident photon beam. Monochromatic light was irradiated at an angle of about 80° to the sample normal to minimize contamination by elastic scattering.

Figure S5 shows sulfur K-edge XANES spectra of AuS (top), SAPd (the second from top) and standard materials. The XANES spectrum of SAPd indicates clear resonance peak at 2481.5 eV. On the other hand, a clear structure cannot be seen at the low energy side. The comparison with the XANES spectra of standard materials suggest that the sulfur contained in SAPd is strongly oxidized and they have the formula of SO_4^{2-}. The XANES spectrum of AuS is almost identical with that of SAPd, and it also shows strong SO_4^{2-} resonance peak. However, we couldn't detect the sulfur signal from Au mesh which has not processed the Pirania treatment. This result indicates that the sulfur contained in SAPd is deposited by Pirania treatment and the chemical form of the adhering sulfur did not change during the following SAPd formation reaction. We can conclude that the origin of sulfur is SO_4^{2-} contained in the sulfuric acid used by Pirania treatment.

XANES spectra of standard material containing SO_4^{2-} are indicated by blue curve. Although both $PdSO_4$ and protamine sulfate include SO_4^{2-} ion, these materials show clearly different spectral profiles. Whereas protamine sulfate shows single resonance peak at 2481.5 eV, $PdSO_4$ shows small peak at about 2478.0eV. The shoulder peak was interpreted by the hybridization of S 3p states with the 3d states of the metal cation [10,11]. XANES spectrum of SAPd does not indicate shoulder peak, and spectrum resembles to that of protamine sulfate. The present results suggest that the sulfate and palladium is not present in the form of "$PdSO_4$". This is consistent with the results of EXAFS and TEM analysis. Sulfate could interact closely with the organic matters in SAPd.

The chemical analysis of carbon in SAPd has been carried out at c-branch of BL27SU. At this branch, the photon beam was dispersed by a soft X-ray monochromator with varied-line-spacing plane gratings. XANES spectra were measured by scanning the undulator gap as well as the monochromator scan to maintain maximum intensity of the incident soft X-rays, and by scanning the width of entrance and exit slits to maintain constant resolving power. The higher harmonics of the incident X-rays were reduced using three Cr-coated plane mirrors. The photon energy resolution during the measurements was set at 50 meV. Photon flux on the sample is 1×10^{11} Ph/s at 0.3keV (carbon K-edge). To analyse carbon XANES spectra, palylene-N and acetic acid palladium(II) were chosen as a standard material. Palylene-N is a polymer of the *p*-xylene which is used in Pd adsorption process. All of the spectra were measured by total electron yield method. In order to eliminate the artifacts appearing in XANES spectra due to the carbon contamination of optical elements, the correct intensity curve of the incoming photon (*I0*) was measured by using Si-PIN photodiode detector after the XANES measurement of samples.

Figure S6 shows the C K-edge XANES spectra of SAPd and standard materials. Top spectrum shows XANES spectrum of SAPd, and bottom spectra show the XANES spectra of

standard materials. These standard specimens are the primary materials of SAPd, as was described above. Peak assignments are made by comparison with previous XANES studies of corresponding materials [12,13], and the assignments are shown in the Figure. Remarkable feature can be found at about 285.0 eV. It is well known that this peak appears in the C K-edge XANES spectra of graphite where carbon atoms has sp2 hybridization and out-of-plane π bonds, but not in that of diamond with only sp3 hybridization [14]. Therefore, the peaks at 285 eV are due to the electronic transition from C 1s to π* orbital and is a measure of the presence of conjugated bond in aromatic ring. On the other hand, the spectral features are independent of the angle between the polarization vectors of incident X-ray beam [14]. The independence suggests that the aromatic rings are randomly oriented in SAPd sample. When we discuss about the carbon chemical state based on the primary materials of SAPd, one conceivable model is that the aromatic rings have phenyl structure and connected by CH_2 groups. The phenyl rings could be produced by *p*-xylene which is a solvent of a Pd nano-cluster formation. This interpretation can be supported from the experimental fact that XANES spectrum of SAPd is resembled to that of palylene-N. The origin of aromatic ring is expected to be prepared from the *p*-xylene.

Although XANES spectrum of SAPd and palylne-N are similar, there are two clear differences. First is that the π* excitation peak at 285 eV of palylne-N shows double peak structure. On the other hand, the intensity of higher peak is slightly suppressed in the spectrum of SAPd. It is well known that the resonance energy and peak shape of the π* excitation depends on the other neighbors of the excited carbon atoms. For example, when all carbon atoms in aromatic ring are equivalent, e.g., benzene, the XANES spectrum shows single resonance peak at around 285 eV [15]. On the other hand, carbon atom with a certain functional group indicates the shift of resonance energy and the resonance peak split into several peaks. Judging from these knowledges, whereas the higher energy peak originates from the excitation of carbon atom on the phenyl rings connected by CH_2, carbon atoms having less interaction with neighboring atoms around the aromatic ring show lower energy peak. The suppression of higher energy peak intensity suggests that the chain length of aggregated xylene is shorter than pure palylene-N polymer. The second difference is that the peak at 288.0eV is enhanced than that of palylene-N. This enhancement can be interpreted by the existence of carbonyl group in SAPd. In the SAPd synthesis processes, Pd atom is added by acetic acid palladium(II). The bottom spectrum of S6 is the XANES spectrum of acetic acid palladium(II), and we can confirm π*(C=O) resonance peak at 288.0eV.

When we discuss about the carbon atoms in SAPd based on the primary materials of SAPd, one conceivable model is that the xylene forms a chain of phenyl rings connected by CH_2 and/or CH_3COO, and it constructs the bone structure of SAPd. The phenyl rings could be produced by *p*-xylene which is a solvent of a Pd nano-cluster formation, and carbonyl groups could be produced by

acetic acid palladium(II).

References

1. Hoshiya, N.; Shimoda, M.; Yoshikawa, H.; Yamashita, Y.; Shuto, S.; Arisawa, M. *J. Am. Chem. Soc*. **2010**, *132*, 7270-7272.

2. Swapna, K.; Kumar, A. V.; Reddy V. P; Rao, K. R. *J. Org. Chem*. **2009**, *74*, 7514-7517.

3. T. Honma, H. Oji, S. Hirayama, Y. Taniguchi, H. Ofuchi, M. Takagaki, *AIP Conf. Proc.* **2010**, 1234, 13-16

4. B. Ravel, M. Newville, *J. Synchrotron Rad.* **2005**, 12, 537-541.

5. S. I. Zabinsky, J. J. Rehr, A. L. Ankudinov, R. C. Albers, M. *J. Eller, Phys. Rev. B* **1995**, 52, 2995-3009

6. H. G. Fritsche, R. E. Benfield, Z. *Phys. D* **1993**, 26, 15-27

7. P. V. Menacherry, M. F. Garcia, G. L. Haller, *J. Catal.* **1997**, 166, 75-88

8. J. Stöhr, "NEXAFS Spectroscopy" (Springer, Berlin, 1992).

9. Y. Tamenori, M. Morita and T. Nakamura, *J. Synchrotron Rad.* **18**, 747-752 (2011)

10. N. Okude, M. Nagoshi, H. Noro, Y. Baba, H. Yamamoto and T. A. Sasaki, *J. Electron Spectr. Related. Phonomena.* **101-103**, 607 (1999)

11. M. E. Flett, *Can. Mineral*, **13** 1811 (2005)

12. Y. Ma, H. Yang, J. Guo, C. Sathe, A. Agui and J. Nordgren, *App. Phys. Lett.* **72**, 3353 (1998)

13. B. Watts, S. Swaraj, D. Nordlund, J. Lüning and H. Ade, J. Chem. Phys. 134, 024702 (2011)

14. R. A. Rosenberg, P. J. Love, and V. Rehn, *Phys. Rev.* **B33**, 4034 (1986)

15. C. Kolczewski, R. Püttner, M. Martins, A. S. Schlachter, G. Snell, M. M. Sant'Anna, K. Hermann and G. Kaindl, *J. Chem. Phys.* **124**, 014302 (2006)